NON-STOICHIOMETRIC POLYMER-SURFACTANT COMPLEXES OBTAINED IN A LAMELLAR LYOTROPIC MEDIUM

Yahya Agzenai, Carmen S. Renamayor, Isabel E. Pacios*

Dpt. CC y TT Fisicoquímicas. Facultad de Ciencias, UNED

Pº Senda del Rey 9, 28040 Madrid Spain

Tel/Fax:+34913987390 e-mail: ipacios@ccia.uned.es

Abstract. The addition of a polyelectrolyte to lamellar media formed by an oppositely charged surfactant often leads to the coexistence of several phases without macroscopic phase separation, which makes their characterization difficult. Here, the effect of the polydiallyldimethylammonium chloride (PD) on the lamellar liquid crystal formed by the anionic surfactant Aerosol OT (AOT) and water is investigated. SAXS results are discussed regarding the changes in the lamellar spacing as a function on the PD or AOT concentrations. In most of the samples two lamellar phases, without macroscopic phase separation, are detected. One of them is a typical swollen phase, while the other is a collapsed phase, which corresponds to the polymer-surfactant complex. At concentrations of polymer up to 3 %wt the two lamellar phases coexist, however, at a critical concentration higher than 3 %wt, the swollen phase becomes isotropic, and a macroscopic phase separation takes place. A simple model is proposed to calculate the composition of the phases when macroscopic phase separation does not occur. The results thus calculated show that generally the polymer-surfactant complexes are non-stoichiometric containing a lesser amount of polymer than ideally expected.

Keywords: *SAXS, AOT, polydiallyldimethylammonium chloride, polymer-surfactant complex*

Published in Colloid Polymer Science, vol 290, pp. 1123-1132 (2012)

1. INTRODUCTION

Polymer-surfactant systems have been intensively investigated because they are used in a wide range of applications [1]. In particular, great attention has been paid to the study of charged polymers (polyelectrolytes) and surfactants of opposite charge, because these systems lead to complexes with potential technological applications [2,3] (e.g. medicine [4], cosmetic [5], coatings [6] etc). The polymer surfactant complexes (PSC) are mainly stabilized by electrostatic interactions between the charged surfactant heads and the charged units along the polymer chains, and also by hydrophobic interactions between the polymer backbone and the alkyl tails of the surfactants. As consequence of these two directing forces, PSCs usually present long range order showing different types of organized structures, namely: lamellar [7,8], cubic [9] or hexagonal [10]. The type of structures formed depends on factors such as the global composition [11], the length of the surfactant alkyl chain [12], the length of the polymer chain [13], the charge density of the polyelectrolyte [14] or the presence of co-surfactants [15]. The composition of these complexes is usually assumed to be stoichiometric with equal amounts of the two species of opposite charge [3,6,16,17,18] but in most of the systems studied their detailed stoichiometry has not been characterized and, in a few cases, non-stoichiometric complexes have also been formed [19,20].

Substantial efforts have been made to clarify the formation, properties and structures of PSCs [21,22,23] with theoretical studies [24,25,26] and many experimental studies concerning the incorporation of polyelectrolytes in diluted solutions [10,27] microemulsions [28], solid state [8,29,30] or liquid crystalline systems [31]. More specifically, the incorporation of an oppositely charged polyelectrolyte in a lamellar lyotropic system has been widely studied. These systems are interesting from the fundamental point of view, and for improving the knowledge about biological self-assembling. As an example, it is well known that the interaction between phospholipid bilayers and proteins plays an important role in bio-membranes [32].

As a simpler model, the inclusion of synthetic polyelectrolytes in lamellar lyotropic organizations obtained from synthetic or natural surfactants is usually preferred. In this line Kötz *et al.* have demonstrated that a collapsed lamellar phase is formed when the cationic polymer poly diallildimethylammonium chloride (PD) is incorporated to the lamellar system formed by lecithin and sodium dodecyl sulfate (SDS) in a critical concentration higher than 3 %wt [33]. The collapsed lamellar phase is a non-swollen structure with a constant lamellar spacing independent on the global water content, in which the polymer is adsorbed flat onto the bilayers forming the complex [34,35].

In other works [36,37], it has been proven that PD modifies the lamellar system formed by SDS/decanol/water in a characteristic way: a) at low polymer concentration (up to 1 %wt) the typical swelling behavior of a lamellar phase, increasing the lamellar spacing with the water content, is observed; b) At polymer concentrations higher than 4 %wt only a collapsed lamellar phase is observed; c) At intermediate polymer concentrations, 2–3 %wt, the swollen and the collapsed lamellar phases do coexist. Two lamellar phases have also been detected in other systems [38,39]: According to molecular dynamic simulations, when two lamellar phases are formed, the most part of the polymer is in the phase of the complex but in the swollen phase there are also some polymer molecules in a more folded structure [26]. Nevertheless, the coexistence of two lamellar phases is not well understood and with this purpose more studies have to be done.

The lyotropic system AOT/water forms lamellar mesophases in a wide range of compositions and the incorporation of non-interacting polymers in this system has been intensively studied in our group [40,41]. Here, the effect of the incorporation of PD in the lamellar lyotropic system Aerosol OT/water is studied. As in the systems described above, two phases in equilibrium that do not separate macroscopically coexist. We have investigated their structures by small angle X-ray scattering (SAXS) and optical microscopy. Since these coexisting phases do not separate macroscopically, their compositions remain unknown. One of our goals here is to develop a model which allows us to calculate such composition of the phases and, with it to obtain the stoichiometry of the complexes formed.

2. EXPERIMENTAL PART

2.1. Materials

The surfactant 1,4-bis(2-ethylhexyl)sodium sulfosuccinate (AOT) with 99% purity was purchased from Sigma. Poly(diallyldimethylammonium chloride) (PD) of molecular weights M_w <100,000 (PD1) and M_w 100,000-200,000 (PD2) from Aldrich have been employed: These polymers were provided in water solution and purified by precipitation with ethanol three times. The purified polymers and the AOT were dissolved in water and freeze-dried before used. Deionized water (Milli-Q) was employed for the samples preparation.

2.2.- Sample preparation

Two set of samples were prepared with the two polymers (PD1 or PD2), named sets $PD1_S$, $PD2_S$,

S_{PD1} and S_{PD2}. The sets PD_S-# are formed by six samples having the same PD composition (1.25 wt%) and a surfactant fraction (#) that varies (# = 20, 25, 30, 35, 40 and 45 wt%). The sets S_{PD}-# are formed by seven samples having the same surfactant composition (25 wt%) and a variable weight fraction of PD (# = 0.5, 0.75, 1.25, 2, 3, 4 and 5 wt%). Therefore, there is one sample belonging to both sets (PD_S-25 ≡ S_{PD}-1.25). The final composition of each sample was reached by weighing the proper amounts of AOT, PD and water. Samples were homogenized mixing back and forth for several days. After this process they were allowed to equilibrate at 25 ºC. Additionally, six samples of the binary system AOT/water were prepared with the same surfactant concentration as the set PD_S-#.

2.3. Techniques

Microscopy. A microscope (Nikon Labophot-2) provided with a Nikon camera (model DS-5M) and crossed polarizers was employed to determine the anisotropy of the samples. During these measurements, the samples were placed between a glass slide and a cover slip.

Small Angle X-ray Scattering (SAXS). The experiments were performed at the European Synchrotron Radiation Facility (ESRF) in Grenoble on the beam line BM16. The samples were irradiated with a wavelength λ = 0.979 Å, and two-dimensional images were recorded using a CCD detector (MARCCD 165) with a resolution of 1024 × 1024 pixels, and a pixel size of 159 μm. The sample-detector distance was 1381 mm. Images were integrated to obtain the scattered intensity (I) as a function of the modulus of the scattering vector, $q = (4\pi/\lambda) \sin \theta$, where 2θ is the scattering angle, and were normalized to compensate for the intensity fluctuations of the synchrotron source. Samples were introduced in capillaries and measured in three different locations.

2.4. Polymer characterization

The intrinsic viscosity of the polymers was determined in 1M NaCl water solution at 30 ºC. The solutions of the purified polymers in 1 M NaCl were dialyzed against a salt solution with the same concentration. With this purpose, the polymer solutions were enclosed in dialysis membranes (Spectra/pore) having 10,000 D as molecular mass cut-off and contacted with an excess volume salt solution. In all cases the outer dialysis solutions were also used as solvent in subsequent dilution procedures. Table 1 summarizes the data corresponding to the characterization of the polymers. The intrinsic viscosity was calculated by Huggins and Kraemer extrapolations, and the viscous molecular weight average was calculated by using the Mark-Houwink equation [42] with the exponent a=0.83, and the constant K=4.7×10^{-3} dL/g. The viscosity average molecular weight is usually lower than the

weight average molecular weight, therefore the values obtained agree with the data provided by the producers. The radius of gyration can be estimated using $R_g^2 = C_N N l^2 / 6$. Here the characteristic ratio C_N=17 was obtained from the literature [43], the number of bonds in the main chain, N, was calculated from the polymer molecular weight and l is the bond length (0.154 nm).

Table 1 Intrinsic viscosity, viscosity average molecular weight, density and radius of gyration of PD1 and PD2

	$[\eta]$ (dL/g)	$\overline{M}_v$ (g/mol)	ρ (g/mL)	R_g (nm)
PD1	0.218	2.6×10^4	1.225	6.6
PD2	0.556	8.1×10^4	1.230	11.6

3. RESULTS AND DISCUSSION

3.1. Sample characterization

Mixtures corresponding to set PD_S-# are gel-like, monophasic, white, and present optical anistropy. In the set S_{PD}-#, the samples show the same behaviour when the polymer concentration is lower than 3 wt%, but for higher polymer concentration there is a macroscopic phase separation. The upper phase is an isotropic transparent liquid while the bottom phase is a white solid. There are not significant differences in the macroscopic appearance of the samples with polymer of different molecular weight (PD1 and PD2). As an example samples with PD1 are shown in Fig. **1**.

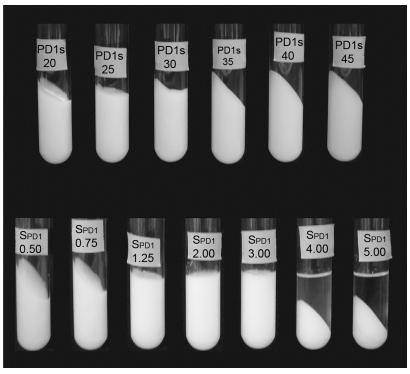

Fig. 1 Pictures of the samples corresponding to the set $PD1_S$-# and S_{PD1}-#

For the samples with polymer, the micrographs without crossed polarizers show a phase separated

pattern which becomes clearer as the polymer concentration increases. With crossed polarizers, optical anisotropy is detected but it is not possible to characterize the texture due to the disturbance produced by the phase separation (Fig. **2**).

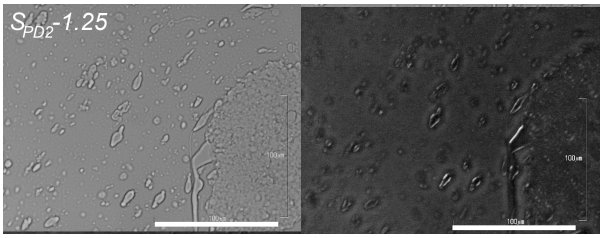

Fig. 2 Micrographs without (left) and with (right) crossed polarizers of sample S_{PD2}-1.25. (Bar = 100μm).

The structural order of the samples studied in this work has been determined from SAXS measurements. Fig. **3** depicts only the pattern of the two sets of samples with the polymer PD1 since there are not significant differences with the PD2.

In the set $PD1_S$-#, the first peak that appears in the diffractogram ($q_1 < 1.5$ nm^{-1}) moves to higher values of the wave vector with the surfactant content. In some of the samples there is other peak in a relative position 1:2. This is characteristic of a swollen lamellar phase (named L). In fact, the pattern is similar to that of the AOT/water lamellar system [44]: (i) there is a broad hump for wave vectors between 1 and 5 nm^{-1} and (ii) for some compositions the second order Bragg peak has higher intensity than the first order diffraction peak and, at a given concentration, the first peak even disappears (here this occurs for the sample $PD1_S$-40). Additionally, there are two other peaks with a relative position of the wave vector 1:2, indicating the coexistence of another lamellar phase. In polymers that do not interact with the surfactant two lamellar phases can also be formed after salt addition, in these cases there is a depletion interaction and the polymer goes to the swollen phase increasing the entropy of the system [45]. In this work, the position of the first diffraction peak slightly diminishes with the surfactant content (2.15-2.19 nm^{-1}) indicating that it is a collapsed phase (named C). It can be associated with the formation of collapsed structures between ionic surfactants and oppositely charged polyelectrolytes. The coulombic interaction gives rise to the formation of complexes where the polymer is adsorbed flat onto the surfactant head groups of the individual bilayers [29], the polyelectrolyte has the effect of bringing oppositely charged surfactant aggregates together, in other words: adsorption cancels depletion. As was explained in the introduction, Kötz *et al.* [36,37] have also reported the coexistence of two lamellar phases, one collapsed and another swollen, when PD is incorporated at a

concentration 2-3 %wt in the lamellar system SDS/decanol/water. Nevertheless, in the AOT/water system this scenario occurs at lower polymer concentration (0.5 %wt) and when the concentration of polymer is higher than 3%, the macroscopic phase separation occurs.

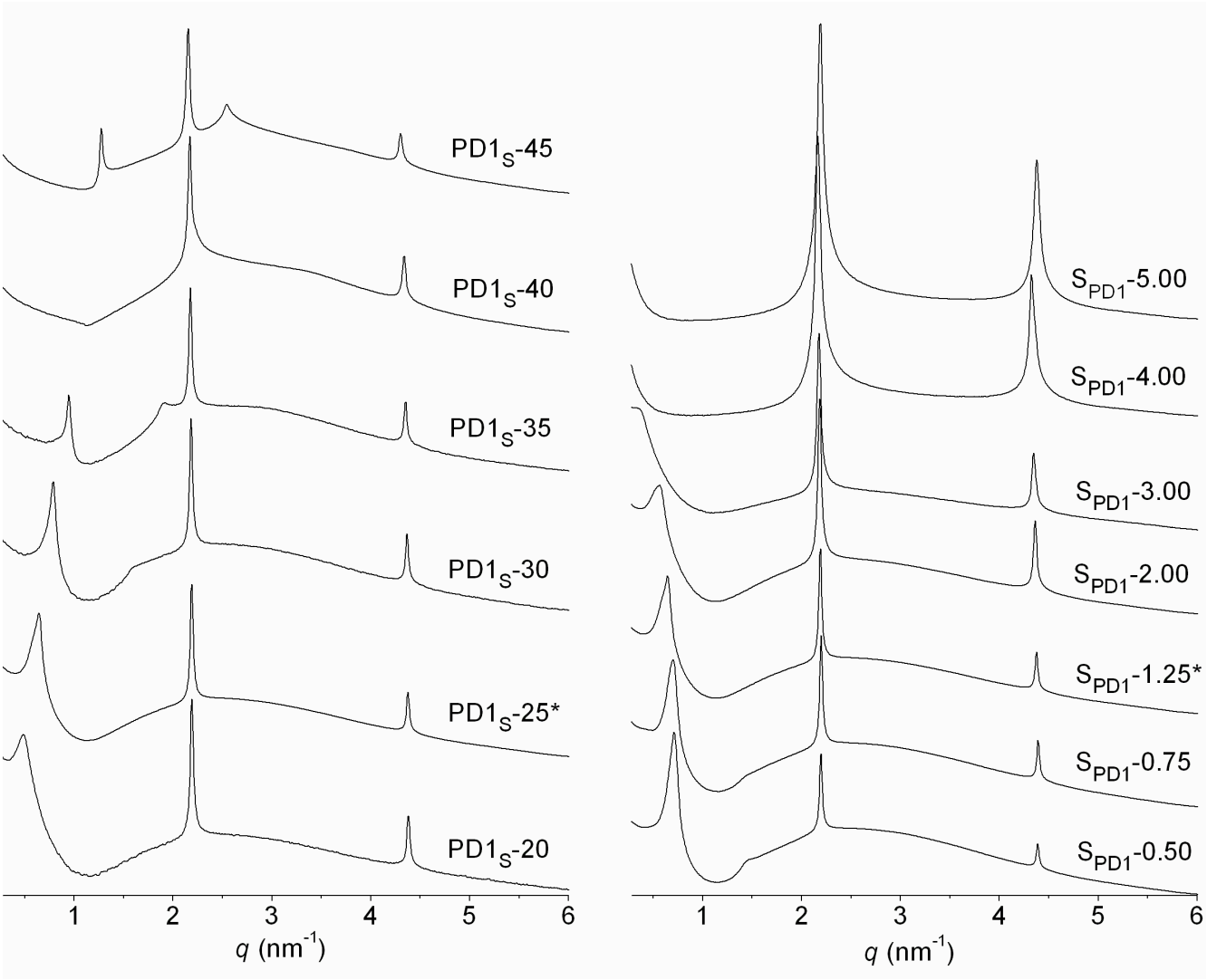

Fig. 3 SAXS diffractograms corresponding to the sets $PD1_S$-# (left) and S_{PD1}-# (right). The diffractograms have been shifted for better visualization. Diffractograms of samples SPD1-4.00 and SPD1-5.00 belong to the bottom macroscopic phases (the upper phases present isotropic diffraction patterns). Intensity in arbitrary units represented in a logarithmic scale. * Diffractograms corresponding to the same sample

In a similar way, in the set S_{PD1}-#, the SAXS pattern corresponding to the samples with polymer concentration lower than 4 %wt shows also the coexistence of a swollen and a collapsed lamellar phase. Nevertheless, for higher polymer concentrations only the collapsed phase is observed. The first

diffraction peak corresponding to the swollen lamellar phase moves to lower values of the wave vector with the polymer content. The position of the peaks characteristic of the collapsed phase slightly decreases with the polymer content (2,20-2,16 nm^{-1}) although their intensity increases significantly with the polymer content (Fig. **3**), which indicates that the amount of the phase of the complex becomes higher.

The long period of the lamellar phase can be calculated from the first order diffraction peak as $d=2\pi/q$. In the diffractograms of the sets of samples in which the surfactant is varied, the peak positions corresponding to the swollen lamellar phase move to higher q values upon increasing the surfactant content. Therefore, the lamellar spacing in this phase, d^L, decreases with the AOT content following a dilution law [46]. In the binary AOT/water system this law can be expressed as $d = d_{AOT} / \phi_{AOT}$, where d_{AOT} is the bilayer thickness and ϕ_{AOT} is the AOT volume fraction. Fig. 4 (left) shows that the presence of polymer induces a small increase in the lamellar spacing of the swollen phase compared with the binary system. This small increase is independent of the polymer molecular weight. In the case of the collapsed lamellar phase of the system PD and sodium dodecyl sulphate, [31] it was not possible to detect any variation of its lamellar spacing, d^C, with the water content. In this work, the accuracy of the measurements, performed with a synchrotron source, allows observing a slight increase of the lamellar spacing of the complexes with the surfactant content. Additionally, a small effect of the molecular weight is observed. The presence of the polymer with the highest molecular weight ($PD2_S$-#) induces a slight decrease of d^C, which suggests a small variation in the complex stoichiometry with the molecular weight.

Fig. **4** (right) depicts also the variation of the long period with the polymer content corresponding to sets S_{PD}-#. In the swollen phase, the addition of polymer produces a strong increase of d^L, that is, the polymer promotes swelling. In the collapsed phase, the lamellar spacing, d^C, slightly increases with the content of PD. In fact, the addition of a small amount of polymer produces a variation of d^C similar than the observer for the PD_S-# series, where the concentration of surfactant strongly varies. In both phases the results suggest also a small effect of the polymer molecular weight.

The results presented above evidence that the presence of polymer induces a phase separation rendering a swollen and a collapsed phase corresponding to the complex. It is expected that the phase of the complex will contain the most part of the polymer [47,48] and a fraction of the AOT and the water, while the swollen phase will be mainly composed by AOT and water. After comparing the lamellar spacing of the phase of the complex (2.8-2.9 nm) with the radius of gyration corresponding to

the polymers PD1 and PD2 (Table 1), it seems evident that the polymer adopts a flat conformation in the complex, in agreement with results on other similar systems [26].

The stoichiometry of the polyelectrolyte-surfactant complex is expected to be 1 to 1, between the negative charge of the head group in AOT and the positive charge per monomer unit in PD. However, this is impossible to prove by direct measurement, when the collapsed phase that holds the complex are not be isolated, because the two coexisting phases do not separate macroscopically. In order to solve this problem, we propose a model that allows an indirect way of determining such a stoichiometry. The model is as follows.

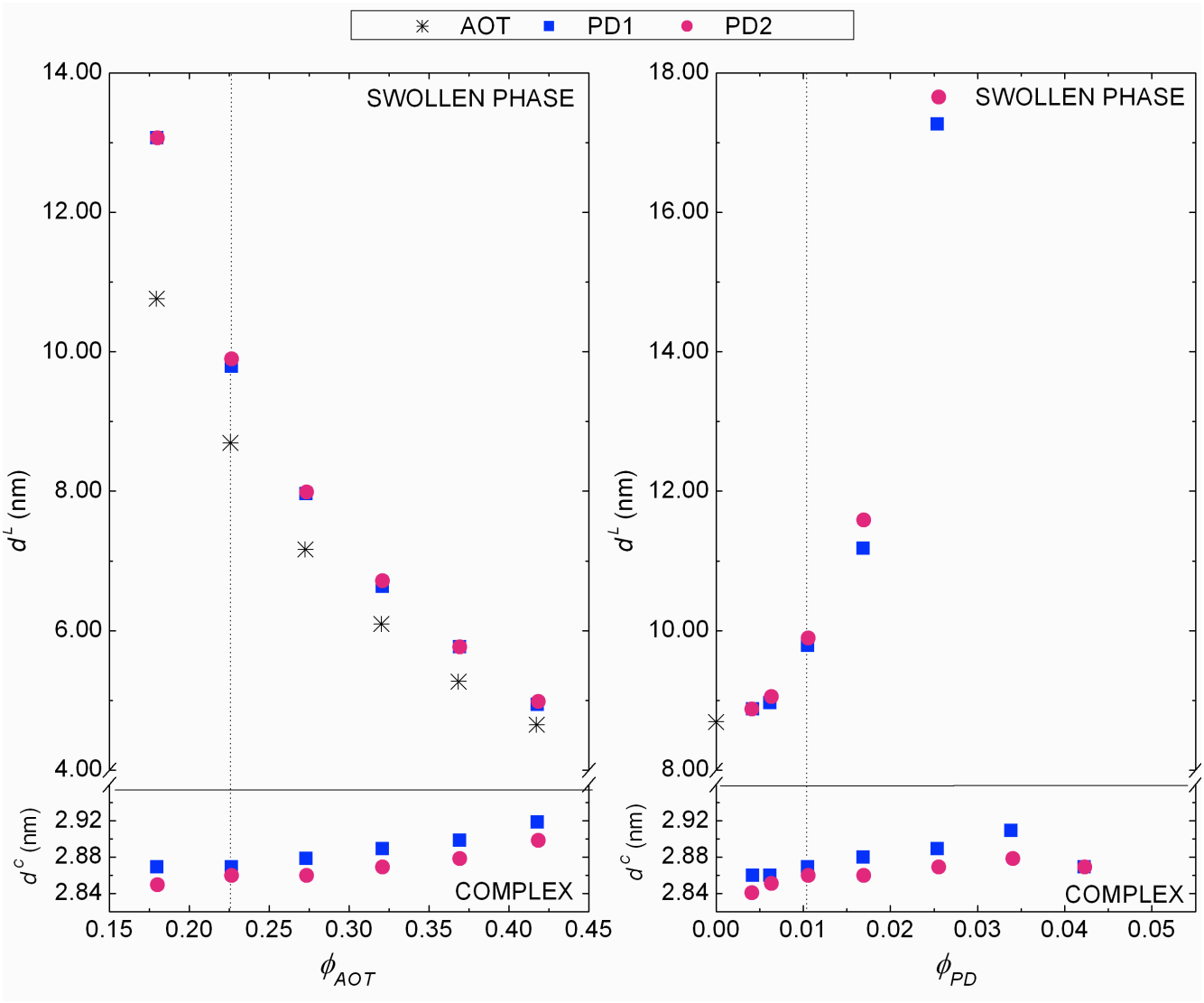

Fig. 4 Lamellar spacing of the two phases determined from SAXS diffractograms. Left side: as a function of Φ_{AOT} for the sets PD_S-#. Right side: as a function of Φ_{PD} for the sets S_{PD}-#. Samples corresponding to the binary AOT/water system are also included. Dotted line points the data corresponding to the common sample in both sets

3.2. The model

We start assuming a given stoichiometry or molar ratio between the monomeric units in the chain and the number of surfactant heads, n_{PD}/n_{AOT}. From this, we calculate the thickness of the complex layer. With this and the experimental spacing between lamellae in the collapsed phase, we can obtain the composition of that phase. Then, from the experimental data of total water and the lamellar spacing in the swollen phase, we can calculate the composition of this phase and the relative volumes of both phases. Once all this is known, we compute the AOT global composition of the sample and compare it with the experimental value. The best value for the stoichiometry of the sample (starting point in the process) is that which gives the minimum difference between the experimental and the calculated global composition. The process is done for each one of the samples. Let us see now the detailed equations used.

Taking into account the lamellar structure of the phase containing the complex, it can be proposed a dilution law for the complex similar to that of the binary AOT/water system. Therefore:

$$d^C = d^* + d_W^C \qquad (1)$$

where d^C is the complex lamellar spacing (determined experimentally), d^* represents the thickness of the PD/AOT complex without water and d_W^C represents the water layer thickness. In the same way, it is assumed that the PD charged units flat-adsorbed onto the AOT bilayers have a characteristic thickness, d_{PD}, then:

$$d^* = d_{AOT} + d_{PD} \qquad (2)$$

where d_{AOT}=1.95 nm, obtained from the binary AOT/water system [46].

In the lamellar complex the ratio between d_{PD} and d_{AOT} is equivalent to the ratio between the volumes of the oppositely charged units in the collapsed phase (V_{PD}^C and V_{AOT}^C):

$$\frac{d_{PD}}{d_{AOT}} = \frac{V_{PD}^C}{V_{AOT}^C} \qquad (3)$$

Additionally, this ratio can be expressed as a function of the molar ratios of the charged units

(n_{PD}/n_{AOT}) and their molecular weights (M_{PD}/M_{AOT}) as:

$$\frac{V_{PD}^{C}}{V_{AOT}^{C}} = \frac{\rho_{AOT} M_{PD}}{\rho_{PD} M_{AOT}} \frac{n_{PD}}{n_{AOT}} \qquad (4)$$

where the density of AOT (ρ_{AOT} = 1.14 g/mL) is obtained from bibliography [49] and the densities of PD have been experimentally determined (Table 1)

The volume of the phase of the complex (V^{C}) is given by:

$$V^{C} = V_{PD}^{C} + V_{AOT}^{C} + V_{w}^{C} \qquad (5)$$

where V_{w}^{C} is the water volume in the phase of the complex. After dividing by V^{C}, equation (4) renders:

$$\frac{V_{PD}^{C}}{V_{AOT}^{C}} = \frac{\varphi_{PD}^{C}}{\varphi_{AOT}^{C}} \qquad (6)$$

where φ_{PD}^{C} and φ_{AOT}^{C} are the volume fractions corresponding to the PD and AOT units in the phase of the complex. From equations (2), (3) and (6), it can be obtained:

$$d^{*} = d_{AOT}\left(1 + \frac{\varphi_{PD}^{C}}{\varphi_{AOT}^{C}}\right) \qquad (7)$$

Once the value of *d** is known, it is possible to estimate d_{w}^{C} with the equation (1). Therefore, the water volume fraction in this phase, φ_{w}^{C} can be obtained as:

$$\varphi_{w}^{C} = \frac{d_{w}^{C}}{d^{C}} \qquad (8)$$

On the other hand, the expression:

$$\varphi_{PD}^{C} + \varphi_{AOT}^{C} + \varphi_{w}^{C} = 1 \qquad (9)$$

can be transformed to give:

$$\varphi_{AOT}^{C} = \frac{1-\varphi_{w}^{C}}{1+\frac{\varphi_{PD}^{C}}{\varphi_{AOT}^{C}}} \qquad (10)$$

Which allows determining φ_{AOT}^{C}, since φ_{w}^{C} and $\varphi_{PD}^{C}/\varphi_{AOT}^{C}$ were previously calculated. Finally, φ_{PD}^{C} can be obtained as:

$$\varphi_{PD}^{C} = 1-\varphi_{AOT}^{C}-\varphi_{w}^{C} \qquad (11)$$

Therefore, the composition of the phase of the complex has been estimated as a function of the ratio n_{PD}/n_{AOT} in this phase.

It is also possible to obtain the volume ratio between a given phase (V^L or V^C) and the total volume. With this purpose the next expression, which relates the global water volume fraction (ϕ_w) to the water volume fraction in both phases (φ_{w}^{C} and φ_{w}^{L}), is employed:

$$\phi_w = \varphi_{w}^{C}\frac{V^C}{V_T} + \varphi_{w}^{L}\frac{V^L}{V_T} \qquad (12)$$

Given that the total volume is $V_T = V^L + V^C$, equation (12) can be expressed as:

$$\frac{V^L}{V_T} = \frac{\phi_w - \varphi_{w}^{C}}{\varphi_{w}^{L} - \varphi_{w}^{C}} \qquad (13)$$

The volume fraction of AOT in the swollen phase is obtained as:

$$\varphi_{AOT}^{L} = \frac{d_{AOT}}{d} \qquad (14)$$

Therefore, for calculation in equation (13), it can be considered that $\varphi_{w}^{L} \approx 1 - d_{AOT}/d$, since the polymer concentration is small compared to the water content.

Once it is known the ratio V^L/V_T and the composition of the phase of the complex, it can be determined the polymer and water concentration in the swollen phase as follows:

The volume fraction of PD, φ_{PD}^{L}, is calculated from:

$$\varphi_{PD}^{C}\frac{V^{C}}{V_T}+\varphi_{PD}^{L}\frac{V^{L}}{V_T}=\phi_{PD} \qquad (15)$$

and the volume fraction of water in the swollen phase, φ_w^L is calculated as:

$$\varphi_w^L = 1-\varphi_{AOT}^{L}-\varphi_{PD}^{L} \qquad (16)$$

Finally, as a method for controlling the validity of the model and the stoichiometry proposed, the global AOT volume fraction is calculated. This calculated value, ϕ_{AOT}^{T}, is obtained as:

$$\phi_{AOT}^{T}=\varphi_{AOT}^{C}\frac{V^{C}}{V_T}+\varphi_{AOT}^{L}\frac{V^{L}}{V_T} \qquad (17)$$

This calculated ϕ_{AOT}^{T} is then compared with the experimental one (ϕ_{AOT}). For each sample, the stoichoimetry of the complex is changed until the difference between ϕ_{AOT}^{T} and the experimental value, ϕ_{AOT}, is minimized.

3.2.1 Composition of the phases

With the method explained above, it has been obtained the stoichiometry for the complex formed between PD and the AOT. The results are presented in Fig. 5, where it is depicted the stoichiometry *vs.* the polymer/AOT molar ratio employed in the preparation of the samples (N_{PD}/N_{AOT}). It can be observed that these complexes are non-stoichiometric and the stoichiometry varies with the sample compositions. The similarity of the values obtained for PD1 and PD2 series suggests that the molecular weight does not influence significantly the stoichiometry, at least in the range of molecular weights studied here.

In the S_{PD} series (filled symbols) the total concentration of surfactant is constant and, therefore, when the polymer concentration increases, N_{PD}/N_{AOT} also increases. The figure shows that, in these series, the addition of polymer increases the amount of surfactant in the complex. To understand this odd result, it should be taken into account that the adsorption of the polymer onto the surfactant bilayer is accompanied by a loss of entropy, which is compensated by the release of Na^+ and Cl^- ions to the medium (Na^+ from AOT, Cl^- from PD); consequently a significant increase of the ionic strength occurs. The effect of the ionic strength in the stoichiometry of PSCs was previously studied, and it was

observed that the salt addition induces the formation of complexes with higher surfactant content [19]. Our present results for series S follow this same trend.

On the other hand, in the series PD_S-# the polymer concentration is constant and the surfactant concentration varies, therefore when surfactant content increases along the series, the ratio N_{PD}/N_{AOT} diminishes. Fig. 5 shows that, as expected, in these series the addition of surfactant drives to complexes with higher AOT content. In these samples, the effect of the ionic strength is negligible because the polymer concentration is almost constant, and consequently the salt amount released to the medium (Cl^- and Na^+) when the complexes are formed, should be approximately the same. Therefore, in this case, the stoichiometry is governed by the excess of surfactant.

Non-stoichiometric complexes have also been reported for other systems. It has been shown that in the mixtures of cetyltrimethylammonium bromide with cetyltrimethylammonium polyacrylate, a concentrated hexagonal phase separates out from aqueous mixtures, showing a strong variation of the surfactant/polyacrylate ratio [50]. Another work by the same group also depicts variations in the stoichiometry of the complexes [51]. It has been also found that PD forms with sodium dodecylsulphate complexes with a 20-30 % of surfactant excess [20].

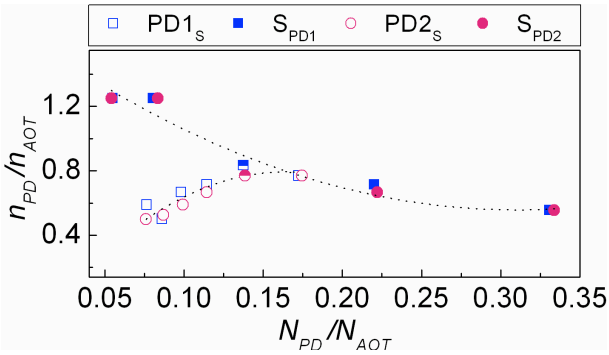

Fig. 5 Stoichiometry of the complexes formed between the polymers (PD1, PD2) and the AOT as a function of the polymer/AOT molar ratio obtained from the global composition of each sample (N_{PD}/N_{AOT}). Half filled symbols correspond to the sample belonging to both sets. Dotted lines are drawn only as eye guides

Fig. **6** depicts the composition of the swollen and complex phases obtained with the model proposed above. The swollen phase, L, is mainly composed by AOT and water, being the concentration of polymer practically negligible. Additionally, the following features can be observed:

(i) The samples $PD1_S$-# and $PD2_S$-# show the typical swelling behavior: the water content decreases with the global AOT volume fraction.

(ii) In the series S_{PD1}-# and S_{PD2}-#, the AOT concentration diminishes with the global polymer

concentration, as expected, because the polymer goes to the phase of the complex taking with it an important part of the AOT. In fact, the swollen lamellar phase can only be observed for the samples with a global polymer volume fraction lower than 0.025. At higher polymer concentrations this phase becomes isotropic and the macroscopic phase separation occurs.

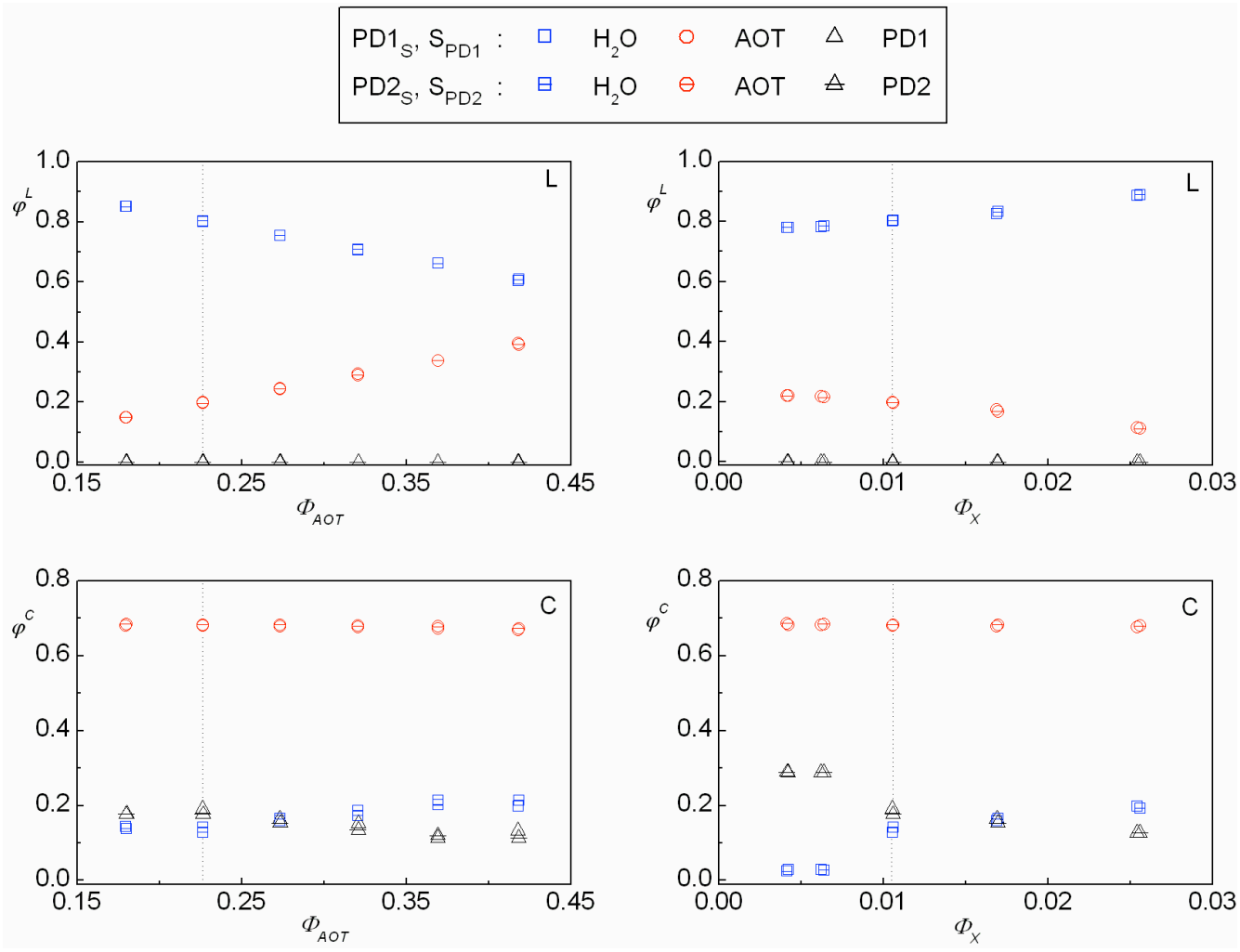

Fig. 6 Composition of the swollen phases, L (up), and the phases of the complex, C (down). On the left, effect of the variation of the global AOT volume fraction: $PD1_S$-# and $PD2_S$-# series. On the right, effect of the variation of the global polymer volume fraction: S_{PD1}-#, and S_{PD2}-# series. Dotted line points the data corresponding to the common sample in both sets

The main component of the phase of the complex is the AOT, and its concentration does not vary significantly, either in the series PD_S-# or S_{PD}-#.

The water concentration in phase C increases with the global content of surfactant, for PD_S-# series, and with the global content of polymer for the S_{PD}-# series, while the polymer concentration of phase C

exhibits the opposite trend. This apparently unexpected result for the serie S_{PD}-# can be explained taking into account the variation of the ionic strength in these samples, which produces a change in the stoichiometry enriching the surfactant content in the complex, as was indicated above. The screening produced by the salt diminishes the effective charge density, which can lead to a conformational change of the polymer molecule [25] that would explain the change in the stoichiometry of the complex.

As was previously explained, there is not macroscopic phase separation in most of the samples. Nevertheless, the model allows obtaining the volume fraction of the swollen lamellar phase (V^L/V_T) Fig. **7** shows that V^L/V_T diminishes upon increasing the polymer global volume fraction. According to the model, when the polymer concentration is high enough, most of the AOT goes to the phase of complex and, therefore, its concentration in the swollen phase is very low. Therefore, the swollen lamellar phase disappears becoming isotropic. It can be observed from Fig. **7** that the trend of the theoretical model fits well the experimental values obtained for the samples with an isotropic phase, in which a macroscopic phase separation occurs and, consequently, the volume fraction of swollen phase can be measured. According to this, in the sets of samples where the surfactant concentration varies and the concentration of polymer keeps constant, the proportion of the lamellar swollen phase can be considered constant.

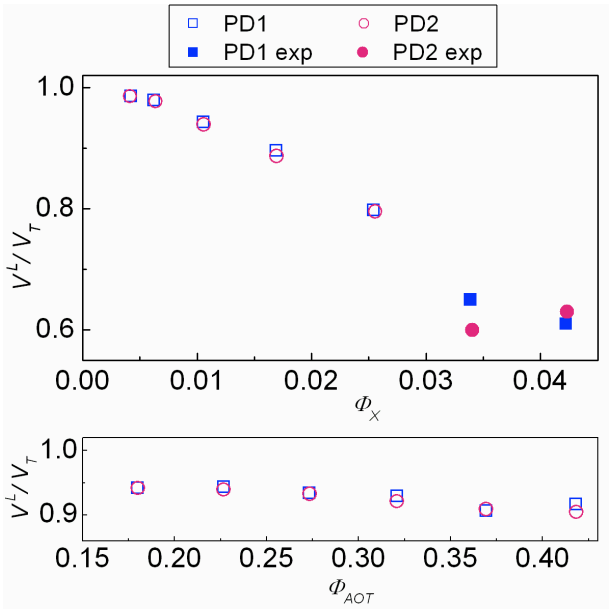

Fig. 7 Volume fraction of the swollen lamellar phase (L). Up: effect of the variation of the global polymer volume fraction: S_{PD1}-#, and S_{PD2}-# series. Down: effect of the variation of the global AOT volume fraction: $PD1_S$-# and $PD2_S$-# series. Open

symbols: values calculated with the model. Closed symbols: experimental values from samples with macroscopic phase separation

4. CONCLUSIONS

The addition of polydiallyldimethylammonium chloride to the lamellar medium formed by AOT and water induces the segregation in two phases, mostly without macroscopic phase separation. One of the segregated phases corresponds to the complexes formed between the surfactant and the polymer, while the other, in most of the samples, is a typical swollen lamellar phase. The absence of macroscopic phase separation precludes direct determination of the composition of these phases. The model proposed here proves useful in obtaining not only the composition but the volume ratio of these phases and the stoichiometry of the complexes.

The results indicate that these complexes present a variable stoichiometry depending on the composition: 1) when the surfactant content increases the complexes become enriched in this component, as expected; 2) the increase of the polymer concentration enhances the surfactant content in the complexes, due to the rise of the ionic strength, which is produced by the release of Na^+ and Cl^- ions when the complexation takes place; 3) the molecular weight of the polymer does not seem to have influence.

Acknowledgements. This work received financial support from MICINN (Spain), under grant CTQ2919-16414, and from DGUI (Comunidad de Madrid), under R&D Program MODELICO-CM/S2009ESP-1691. We are indebted for beam time in the line BM16 of the ESRF (Grenoble). Prof Arturo Horta is gratefully acknowledged for helpful discussion and advice.

References

1. Jönsson B, Lindman B, Holmberg K, Kronberg B (2003) Surfactant and polymers in aqueous solutions. John Wiley and Sons, U.K.

2. Ober CK, Wegner G (1997) Polyelectrolyte-surfactant complexes in the solid state: facile building blocks for self-organizing materials. Adv Mater 9:17–31

3. Faul CFJ, Antonietti M (2003) Ionic self-assembly: facile synthesis of supramolecular materials. Adv Mater 15:673–683

4. Koltover I, Salditt T, Radler JO, Safinya CR (1998) An inverted hexagonal phase of cationic liposome–DNA complexes related to DNA. Release and Delivery Science 281:78–81

5. Qian L, Charlot M, Perez E, Luengo G, Potter A, Cazeneuve CJ (2004) Dynamic friction by polymer/surfactant mixtures adsorbed on surfaces. Phys Chem B 108: 18608–18614

6. Lochhaas KH, Thünemann AF, Antonietti M (1999) Polyelectrolyte-surfactant complexes with fluorinated surfactants: a new type of material for coatings. Surface Coatings International 9:451–455
7. Harada A, Nozakura S (1984) Formation of organized structures in systems of polyelectrolyte-ionic surfactants. Polym Bull 11:175–178
8. Antonietti M, Conrad J, Thünemann A (1994) Polyelectrolyte-surfactant complexes: a new type of solid, mesomorphous material. Macromolecules 27:6007–6011
9. a) Sokolov EL, Yeh F, Khokhlov A, Chu B (1996) Nanoscale supramolecular ordering in gel-surfactant complexes: sodium alkyl sulfates in poly(diallyldimethylammonium chloride). Langmuir 12:6229–6234. b) Sokolov EL, Yeh F, Khokhlov A, Grinberg VY, Chu B (1998) Nanostructure formation in polyelectrolyte-surfactant complexes. J Phys Chem B 102:7091–7098
10. Ilekti P, Martin T, Cabane B, Piculell L (1999) Effects of polyelectrolytes on the structures and interactions of surfactant aggregates. J Phys Chem B 103:9831–9840
11. Leonard MJ, Strey HH (2003) Phase diagrams of stoichiometric polyelectrolyte-surfactant complexes. Macromolecules 36:9549–9558
12. Ponomarenko EA, Tirrell DA, MacKnight WJ (1998) Water-insoluble complexes of poly(L-lysine) with mixed alkyl sulfates: composition-controlled solid state structures. Macromolecules 31:1584–1589
13. Piculell L, Norrman J, Svensson AV, Lynch I, Bernardes JS, Loh W (2009) Ionic surfactants with polymeric counterions. Adv Colloid Interface Sci 147-148:228–236
14. Merta J, Torkkeli M, Ikonen T, Serimaa R, Stenius P (2001) Structure of cationic starch (CS)/anionic surfactant complexes studied by small-angle X-ray scattering (SAXS). Macromolecules 34:2937–2946
15. Bernades JS, Piculell L, Loh W (2011) Self-assembly of polyion–surfactant ion complex salts in mixtures with water and *n*-alcohols. J Phys Chem B 115:9050–9058
16. Vincekovic M, Pustak A, Tušek-Bozic LJ, Liu F, Ungar G, Bujan M, Šmit I, Filipovic-Vincekovic NJ (2010) Structural and thermal study of mesomorphic dodecylammonium carrageenates. Colloid Interface Sci 341:117–123
17. Macdonald PM, Strashko V (1998) A thermotropic phase transition in polyelectrolyte-surfactant complexes as characterized by deuterium NMR. Langmuir 14:4758–4764
18. Yu Q, Frömmel J, Wolff T, Procházka K (2004) Ionene–surfactant complexes: temperature and humidity sensitive materials. Colloid Polym Sci 282:1039–1043
19. Mironov AV, Starodoubtsev SG, Khokhlov AR, Dembo AT, Yakunin AN (1998) Ordered nonstoichiometric polymer gel−surfactant complexes in aqueous medium with high ionic strength. Macromolecules 31:7698–7705
20. Carnali JO, Shah PJ (2008) Correlation of surfactant/polymer phase behavior with adsorption on target surfaces. Phys Chem B 112:7171–7182
21. Antonietti M, Thünemann A (1996) Polyelectrolyte-lipid complexes as membrane mimetic systems**.** Curr Opin Colloid Interface Sci 1:667–671
22. Goddard ED, Ananthapadmanabhan KP (1993) Interaction of Surfactants with Polymers and Proteins. CRC Press, Boca Raton

23. Thünemann AF (2002) Polyelectrolyte–surfactant complexes (synthesis, structure and materials aspects). Prog Polym Sci 27:1473–1572
24. Wallin T, Linse P (1998) Polyelectrolyte-induced micellization of charged surfactants. calculations based on a self-consistent field lattice model. Langmuir 14:2940–2949
25. Ferber C, Löwen HJ (2003) Complexes of polyelectrolytes and oppositely charged ionic surfactants. Chem Phys 118:10774–10779
26. Poghosyan AH, Arsenyan L,H, Gharabekyan HH, Koetz J, Shahinyan AA (2009) Molecular dynamics study of poly(diallyldimethylammonium chloride) (PDADMAC)/sodium dodecyl sulfate (SDS)/decanol/water systems. J Phys Chem B 113:1303–1310
27. Fechner M, Kosmella S, Koetz JJ (2010) pH-dependent polyampholyte SDS interactions. Colloid interface Sci 345:384–391
28. Koetz J, Günther C, Kosmella S, Kleinpeter E, Wolf G (2003) Polyelectrolyte-induced structural changes in the isotropic phase of the sulfobetaine/pentanol/toluene/water system. Progr Colloid Polym Sci 122:27–36
29. Kharas GB, Heiskell JR, Herrman J, Kasudia PT, Schreiber PJ, Passe LB, Bravo-Grimaldo E, Bazuin CG, Romanowski PT, Schueller RM (2006) Solid-state polyelectrolyte complexes of branched poly(ethylenimine) and sodium lauryl sulfate. J Macromol Sci A 43:213–220
30. Thünemann A, General S (2000) Poly(ethylene imine) *n*-alkyl carboxylate complexes. Langmuir 16:9634–9638
31. Kötz J, Kosmella S, Beitz T (2001) Self-assembled polyelectrolyte systems. Prog Polym Sci 26:1199–1232
32. Marsh D, Horvath LI, Swamy MJ, Mantripragada S, Kleinschmidt JH (2002) Interaction of membrane-spanning proteins with peripheral and lipid-anchored membrane proteins: perspectives from protein-lipid interactions. Mol Membrane Biol 19:247–255
33. Robertson D, Hellweg T, Tiersch B, Koetz JJ (2004) Polymer-induced structural changes in lecithin/sodium dodecyl sulfate-based multilamellar vesicles. Colloid Interface Sci 270:187–194
34. Ficheux MF, Bellocq AM, Nallet F (1997) Effect of two water-soluble polymers on the stability of the AOT-H_2O-lamellar phase. Colloids Surf A 123-124:253–263
35. Deme B, Dubois M, Zemb T, Cabane B (1996) Effect of carbohydrates on the swelling of a lyotropic lamellar phase. J Phys Chem 100:3828–3838
36. Koetz J, Kosmella S (1997) Polymers in lyotropic liquid crystalline systems. Colloids Surf A 123-124:265–276
37. Hellweg T, Brûlet A, Lapp A, Robertson D, Kötz J (2002) Temperature and polymer induced structural changes in SDS/decanol based multilamellar vesicles. Phys Chem Chem Phys 4:2612–2616
38. Ruppelt D, Kötz J, Jaeger W, Friberg SE, Mackay RA (1997) Influence of cationic polyelectrolytes on structure formation in lamellar liquid crystalline systems. Langmuir 13:3316–3319
39. Khandurina YV, Alexeev V, Evmenenko GA, Dembo AT, Rogacheva VB, Zezin AB (1995) On the structure of polyacrylate-surfactant complexes. J Phys II France 5:337–342

40. Pacios IE, Renamayor CS, Horta A, Lindman B, Thuresson K (2005) Fragmentation of the lamellae and fractionation of polymer coils upon mixing poly(dimethylacrylamide) with the lamellar phase of aerosol OT in water. J Phys Chem B 109: 23896–23904

41. Pacios IE, Renamayor CS, Horta A, Lindman B, Thuresson K (2002) Equilibrium between poly(*N,N*-dimethylacrylamide) and the lamellar phase of aerosol OT/water. J Phys Chem B 106:5035–5041

42. Dautzenberg H, Görnitz E, Jaeger W (1998) Synthesis and characterization of poly(diallyldimethylammonium chloride) in a broad range of molecular weight. Macromol Chem Phys 199:1561–1571

43. Marcelo G, Tarazona MP, Saiz E (2005) Solution properties of poly(diallyldimethylammonium chloride). Polymer 46:2584–2594

44. Nallet F, Laversanne R, Roux D (1993) Modelling X-ray or neutron scattering spectra of lyotropic lamellar phases: interplay between form and structure factors. J Phys II 3:487–502

45. Ligoure C, Bouglet G, Porte G, Diat O (1997) Smectic compressibility of polymer-containing lyotropic lamellar phases: an experimental tool to study the thermodynamics of polymer confinement. J Phys II France 7:473–491

46. Fontell K (1973) The structure of the lamellar liquid crystalline phase in aerosol OT–water system. J Colloid Interface Sci 44:318–329

47. Anthony O, Marques CM, Richetti P (1998) Bulk and surface behavior of cationic guars in solutions of oppositely charged surfactants. Langmuir 14:6086–6095

48. Ranganathan S, Kwak JCT (1996) Effect of polymer charge density on the phase behavior of sodium poly(acrylate-co-acrylamide)-DTAB systems. Langmuir 12:1381–1390

49. Ekwall P, Mandell L, Fontell K (1970) Some observations on binary and ternary aerosol OT systems. J Colloid Interface Sci 33:215–235

50. Svensson A, Piculell L, Cabane B, Ilekti P (2002) A new approach to the phase behavior of oppositely charged polymers and surfactants. J Phys Chem B 106:1013–1018

51. Svensson A, Norrman J, Piculell L (2006) Phase behavior of polyion-surfactant ion complex salts: effects of surfactant chain length and polyion length. J Phys Chem B 110:10332–10340

FIGURE CAPTIONS

Fig 1 Pictures of the samples corresponding to the set $PD1_S$-# and S_{PD1}-#

Fig 2 Micrographs without (left) and with (right) crossed polarizers of sample S_{PD2}-1.25. (Bar = 100μm).

Fig 3 SAXS diffractograms corresponding to the sets $PD1_S$-# (left) and S_{PD1}-# (right). The diffractograms have been shifted for better visualization. Diffractograms of samples SPD1-4.00 and

SPD1-5.00 belong to the bottom macroscopic phases (the upper phases present isotropic diffraction patterns). Intensity in arbitrary units represented in a logarithmic scale. * Diffractograms corresponding to the same sample

Fig 4 Lamellar spacing of the two phases determined from SAXS diffractograms. Left side: as a function of Φ_{AOT} for the sets PD_S-#. Right side: as a function of Φ_{PD} for the sets S_{PD}-#. Samples corresponding to the binary AOT/water system are also included. Dotted line points the data corresponding to the common sample in both sets

Fig 5 Stoichiometry of the complexes formed between the polymers (PD1, PD2) and the AOT as a function of the polymer/AOT molar ratio obtained from the global composition of each sample (N_{PD}/N_{AOT}). Half filled symbols correspond to the sample belonging to both sets. Dotted lines are drawn only as eye guides

Fig 6 Composition of the swollen phases, L (up), and the phases of the complex, C (down). On the left, effect of the variation of the global AOT volume fraction: $PD1_S$-# and $PD2_S$-# series. On the right, effect of the variation of the global polymer volume fraction: S_{PD1}-#, and S_{PD2}-# series. Dotted line points the data corresponding to the common sample in both sets

Fig 7 Volume fraction of the swollen lamellar phase (L). Up: effect of the variation of the global polymer volume fraction: S_{PD1}-#, and S_{PD2}-# series. Down: effect of the variation of the global AOT volume fraction: $PD1_S$-# and $PD2_S$-# series. Open symbols: values calculated with the model. Closed symbols: experimental values from samples with macroscopic phase separation

TABLES

Table 1 Intrinsic viscosity, viscosity average molecular weight, density and radius of gyration of PD1 and PD2

	$[\eta]$ (dL/g)	$\overline{M}_v$ (g/mol)	ρ (g/mL)	R_g (nm)
PD1	0.218	2.6×10^4	1.225	6.6
PD2	0.556	8.1×10^4	1.230	11.6